Journal of Manufacturing Processes 29 (2017) 389–398

Contents lists available at ScienceDirect

Journal of Manufacturing Processes

journal homepage: www.elsevier.com/locate/manpro

Technical Paper

Sculpturing of single crystal silicon microstructures by elliptical vibration cutting

Jianguo Zhang[a,b,*], Junjie Zhang[c,**], Tao Cui[a], Zhiwei Hao[d], Ahmed Al Zahrani[e]

[a] Changchun Institute of Optics, Fine Mechanics and Physics, Chinese Academy of Science, Changchun 130033, China
[b] Department of Aerospace Engineering, Nagoya University, Nagoya 464-8603, Japan
[c] Center for Precision Engineering, Harbin Institute of Technology, Harbin 150001, China
[d] Department ofAstronautical and Mechanics, Harbin Institute of Technology, Harbin 150001, China
[e] Department of Mechanical Engineering, University of Jeddah, Jeddah 999088, Saudi Arabia

ARTICLE INFO

Article history:
Received 11 January 2017
Received in revised form 25 June 2017
Accepted 3 September 2017
Available online 9 September 2017

Keywords:
Single crystal silicon
Elliptical vibration cutting
Ductile mode machining
Microstructure
Amplitude-controlled sculpturing

ABSTRACT

Single crystal silicon is necessarily subjected to mechanical precision machining to fulfill its applications in semiconductor and optoelectronics industries. However, brittle defects are inevitably formed on machined surface of intrinsically single crystal silicon. Thus, achieving ductile material removal is critical to obtain ultra-smooth machined surface of single crystal silicon. In the present work, we investigate the feasibility of ductile ultra-precision machining of single crystal silicon by applying the elliptical vibration diamond cutting technology. Grooving experiments demonstrate that silicon micro groove can be successfully formed in ductile mode by employing the elliptical vibration cutting, in contrast to the ordinary cutting that causes serious deterioration of finished surface due to formation of brittle defects. Furthermore, the nominal critical depth of cut for the brittle to ductile transition in the elliptical vibration cutting of single crystal silicon is more than 12 times higher than that in the ordinary cutting. It is found that the extremely small instantaneous uncut chip thickness and small cutting forces in the elliptical vibration cutting are advantageous to suppress crack propagations. Moreover, it is found that the vibration amplitude in the depth of cut direction has a prominent influence on both the nominal critical depth of cut and the machined surface quality. Finally, based on the gained fundamental understanding of brittle to ductile transition mechanisms, two types of high precision silicon microstructures, as sinusoidal grid surface and independent dimple patterns, respectively, are successfully sculptured on single crystal silicon by applying the amplitude-controlled ductile mode sculpturing method with arbitrarily changed depth of cut.

© 2017 The Society of Manufacturing Engineers. Published by Elsevier Ltd. All rights reserved.

1. Introduction

Single crystal silicon (herein referred to as silicon) is a basic technological material in semiconductor and optoelectronics industries for its superior properties of high hardness, high wear resistance, light weight, excellent stability and low oxides formability [1–4]. Recently, silicon microstructures have drawn emerging interests for their applications in high-performance imaging, concentration and illuminationin fields of semiconductors [5,6] and infrared optics [7,8]. While surface integrity in terms of form accuracy and subsurface damage has a strong influence on function and performance of microstructures, the precision manufacturing of silicon microstructures is challenging due to its brittle fracture [3]. The performance of conventional precision grinding and polishing of silicon is greatly limited by initiation and subsequent propagation of cracks, as well as formation of subsurface damages [9–12]. In particular, the ultimate precision polishing for achieving excellent machined surface quality is time consuming and high cost due to its complexity. Additionally, it is also extremely difficult to fabricate sophisticated microstructures with sharp edges in grinding and polishing process. In another hand, although the non-traditional semiconductor lithography technique can be applied in the fabrication of silicon microstructures, it suffers greatly from time consuming and complex operation procedures, high costs of equipment and low precision [13–15]. Therefore, an effective manufacturing technique of low cost, high efficiency, high precision and

* Corresponding author at: Changchun Institute of Optics, Fine Mechanics and Physics, Chinese Academy of Science, Changchun 130033, China.
** Corresponding author at: Center for Precision Engineering, Harbin Institute of Technology, Harbin 150001, China.
E-mail addresses: zhangjg@ciomp.ac.cn (J. Zhang), zhjj505@gmail.com (J. Zhang).

http://dx.doi.org/10.1016/j.jmapro.2017.09.003
1526-6125/© 2017 The Society of Manufacturing Engineers. Published by Elsevier Ltd. All rights reserved.

high surface quality is greatly needed for the fabrication of silicon microstructures.

The ultra-precision diamond cutting technique has been demonstrated to be a promising method for fabrication of surface microstructures, due to its advantages of high geometrical accuracy, high machined surface quality, high machining efficiency, low subsurface damage and high degree of freedom. In particular, the feasibility of ductile cutting of silicon with single crystal diamond (SCD) tool has been investigated experimentally and theoretically over the last few decades. It has been demonstrated that with a depth of cut (DOC) ranging from 50 nm to 250 nm, high machined surface quality of silicon, in terms of nanometric surface finish, submicrometric form accuracy and minimum subsurface damages, can be achieved by ductile cutting [2,4,5,12,16–30]. However, the extremely small DOC utilized in ductile cutting of silicon not only requires extremely high rigidity of ultra-precision machine tools, but also introduces difficulties in realizing uniform ductile cutting of global surface due to the undesired inclination of workpiece surface with respect to workpiece holder and alignment errors of workpice [5,31]. Therefore, improving the nominal critical DOC for ductile cutting is critical to simplify the setting up of ductile cutting of silicon, which also facilitates the industrial applications of low cost precision machine tools.

Over the past decades, the ultrasonic vibration cutting technique has been successfully applied in machining of hard-brittle materials [27–31]. In particular, the machining feasibilities of elliptical vibration cutting (EVC), which was proposed by Shamoto and Moriwaki in 1994 [32], on silicon, tungsten carbide and several other brittle materials with SCD tools were verified [33–37]. For instance, ultra-precision machining of difficult-to-cut materials such as hardened steel [38–40], sintered tungsten carbide [35,36,41], Molybdenum [42], Co-Cr-Mo alloy [43] and Plexiglas [44] were realized by applying the EVC technique. In particular, it is found that the nominal critical DOC for ductile cutting of brittle materials can be greatly increased by applying the EVC, as compared to the ordinary cutting (OC). Zhang et al. [33] presented a specific-cutting-energy-based model to predict the ductile-brittle transition (DBT) in nanomachining of silicon. They theoretically predicted and subsequently experimentally verified the significantly increasing of the nominal critical DOC by applying the EVC. Zhu et al. [34] experimentally confirmed that the nominal critical DOC by applying the EVC is improved to 12.8 times higher than that by the OC. Suzuki et al. [37] carried out a series of micro grooving experiments of brittles materials including sintered tungsten carbide, zirconia ceramics, calcium fluoride and glass, and reported that the nominal critical DOC for ductile cutting can be efficiently improved by applying the EVC. Therefore, the EVC is considered to be a promising manufacturing technology for the precision machining of silicon. However, our fundamental understanding of the mechanisms of ductile cutting of silicon by the EVC is far from being completed. For instance, it is necessary to deeply explore and compare the crack generation in silicon under both the EVC and OC processes, which is advantageous to promoting the ductile machining of silicon in EVC process. Moreover, it is critical to investigate the influence of vibration amplitude in the dynamic EVC process on the ductile cutting of brittle materials. Hence, it is of significant importance to propose a simple prediction criterion to unambiguously indicate the optimal machining conditions for achieving ductile cutting of silicon by using the EVC.

Furthermore, most of previous works focused on the investigation of groove or plane formation, there is rather limited attention paid on the fabrication of functional microstructures by using the EVC. More recently, Chen et al. [5] fabricated micro-pillar and micro-pyramid arrays with nanometric surface finish on silicon through crossed ductile cutting process. Mukaida and Yan [8] fabricated aspherical concave micro lens array on silicon wafer through ductile cutting by applying the slow tool servo diamond turning. The combination of conventional diamond cutting and the fast tool servo (FTS) has also been demonstrated to be effective in the fabrication of silicon microstructures for a variety of applications [45–47]. However, the application of conventional diamond cutting in the fabrication of microstructures on brittle materials is greatly hindered by its low efficiency or complexity. Suzuki et al. [48] recently proposed a unique micro/nano sculpturing method by controlling the vibration amplitude in the EVC process, which is capable of achieving high efficient fabrication of high accuracy microstructures on the hard brittle and other difficult-to-cut materials. In the proposed method, the elliptical vibration amplitude is actively controlled during the ongoing machining process, which enables rapid changes of DOC without the utilization of FTS technology. It is suggested that the EVC technology is already equipped with a FTS function itself. Therefore, the EVC can attract increasing attention in the precision micro/nano machining of brittle materials for its feasibility of fabrication of silicon microstructures through ductile cutting, which is helpful to promote the industrial application of the EVC technology in micro/nano machining of the functional silicon structures.

In the present work, grooving experiments are firstly carried out to investigate the machinability of silicon in the EVC and OC, with an emphasis on the ductile cutting mechanisms of silicon under the EVC. Experimental results show that the nominal critical DOC for the DBT in the EVC is 12 times higher than that in the OC. Furthermore, the machinability of silicon with respect to vibration conditions is also investigated, and a simple criterion is proposed to indicate optimal machining conditions for achieving ductile cutting of silicon in the EVC. Subsequently, high precision silicon microstructures, as grid surface and dimple patterns with sinusoidal and triangular cross-section shapes, respectively, are successfully fabricated in ductile mode by applying the EVC, demonstrating the feasibility of the EVC for the high efficiency fabrication of silicon microstructures. The paper is structured as follows. Section 2 introduces the principle of the EVC and experimental setup. Section 3 presents the comparison of grooving machining results of silicon between the EVC and the OC, and the DBT mechanism is also discussed. Section 4 shows the fabrication of silicon microstructures. Finally, Section 5 summarizes the findings found in the present work.

2. Experimental methods

2.1. Principle of EVC

Fig. 1 schematically illustrates the EVC process that was originally presented by Shamoto et al. [49,50]. The nominal cutting direction and the DOC direction is parallel to x axis and z axis, respectively. In the EVC process, the cutting tool is fed at a nominal cutting speed v_c, and the tool edge is controlled to vibrate elliptically at an angular frequency ω in the x-z plane. The tool trajectory in the course of EVC can be expressed as follows:

$$x_e = A_c\cos(\omega\tau) + v_c\tau, \tag{1}$$

$$z_e = A_d\cos(\omega\tau+\varphi), \tag{2}$$

where x_e and z_e denotes x and z component of a relative position between the tool and workpiece, respectively. A_c and A_d is mean-to-peak amplitude in x and z direction, respectively. φ is a phase shift of the vibration, which is typically set to be -90°. τ is the time during the elliptical vibration process.

As illustrated in Fig. 1, the tool starts to cut the workpiece at time t_1 in each elliptical vibration cycle. Subsequently, the workpiece material is removed in the form ofchips until the tangential direction of the tool trajectory is parallel to the rake face, at which

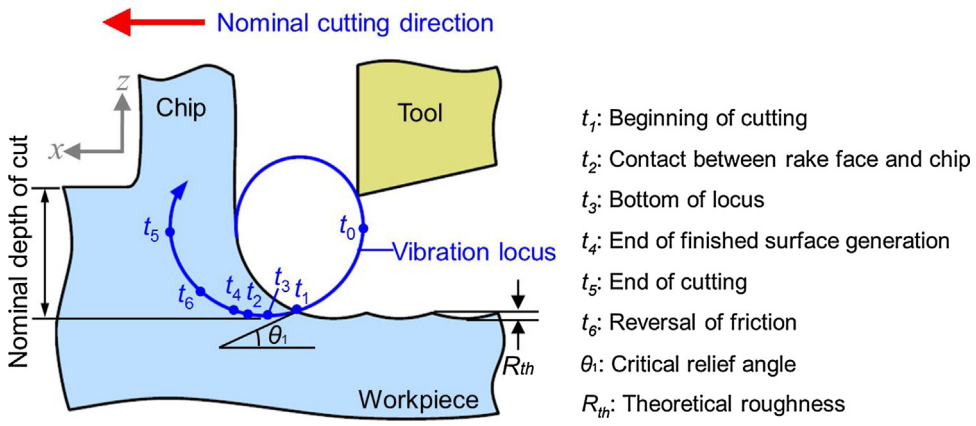

Fig. 1. Schematic illustration of elliptical vibration cutting process [49,50].

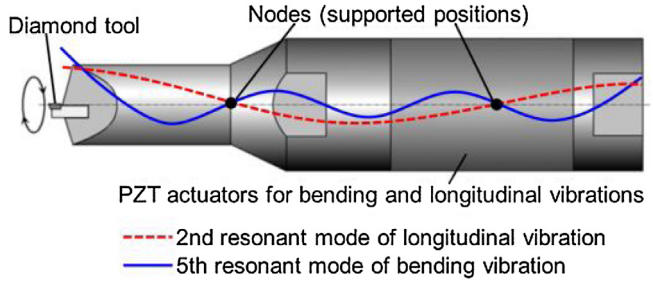

Fig. 2. Ultrasonic elliptical vibrator with longitudinal and bending modes [51].

the cutting tool separates from the chip at t_5. To ensure the complete separation of the tool from the workpiece in each vibration cycle, the nominal cutting speed is lower than the maximum vibration speed in the nominal cutting direction. Additionally, the tool cuts the surface that has been finished in the former vibration cycle, which means that the actual uncut chip thickness in each vibration cycle is smaller than the nominal DOC. Moreover, due to the tool-workpiece separation in each vibration cycle, the contacted surfaces of both the tool edge and the workpiece can be exposed into surrounding gas and/or cutting fluid, and resulting cooling effect efficiently suppresses both thermo-chemical, adhesion and diffusion wear.

2.2. Cutting setup

In the present study, the workpiece is a commercially available single crystal (100) silicon wafer with a chemo-mechanical polished finish. The wafer has a dimension of 50 mm in diameter and 0.5 mm in thickness. The utilized SCD tool has a nose radius of 1 mm, a clearance angle of 10° and a rake angle of 0°. Both crystal orientations of the flank face and the rake face of the SCD tool are (100). An ultra-precision machine tool ATC-400, made by LT Ultra-Precision Technology GmbH with a positioning resolution of 10 nm, is used for performing the cutting experiments. A two-degree-of-freedom (2-DOF) elliptical vibrator, which is capable of generating arbitrary elliptical vibrations within 0-2 μm mean-to-peak amplitudes, is used. The vibrator is actuated by exciting PZT actuators that are sandwiched with metal cylindrical parts. Since the vibrator has the same resonant frequencies in the second resonant mode of longitudinal vibration and the fifth resonant mode of bending vibration, simultaneous longitudinal and bending vibrations at the same ultrasonic frequency of about 41.6 kHz can be achieved. Consequently, a 2-DOF elliptical vibration can be obtained at the diamond tool tip, as shown in Fig. 2 [51].

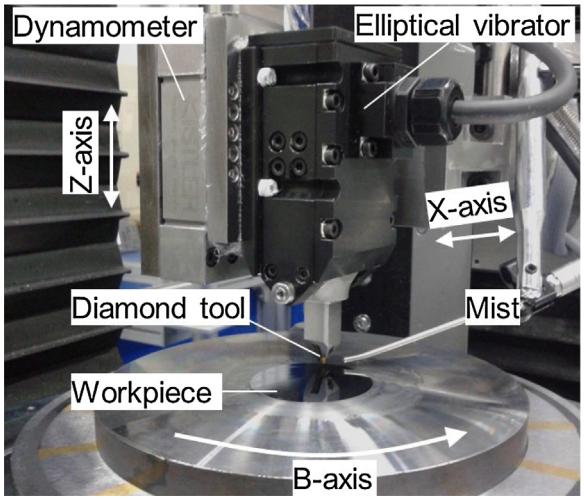

Fig. 3. Experimental set up of the EVC.

Table 1
Experimental conditions in grooving experiments.

Elliptical vibration conditions	Frequency [kHz]	41.6
	Amplitude in nominal cutting direction [$\mu m_{0\text{-}p}$]	2
	Amplitude in depth of cut direction [$\mu m_{0\text{-}p}$]	0.5-2
	Phase shift [deg]	-90
Cutting conditions	Depth of cut [μm]	0-maximum 2.5
	Nominal cutting speed [mm/min]	200
	Cutting fluid (oil moistening)	Kerosene

Fig. 3 shows that in the experimental setup the vibrator and the workpiece is fixed to the Z axis table and the top surface of the B-axis rotation table, respectively. The DOC in each grooving experiment is linearly increased from 0 to 2.5 μm to address the DOC dependence of the machining. The experimental conditions are summarized in Table 1.

3. Fundamental grooving experiments

3.1. EVC versus OC

Grooving experiments under the EVC and the OC are first performed to obtain the first impression of machinability of silicon. For each type of cutting process, the nominal DOC is increased from 0 to the maximum value of 2.5 μm, while the cutting speed is fixed as

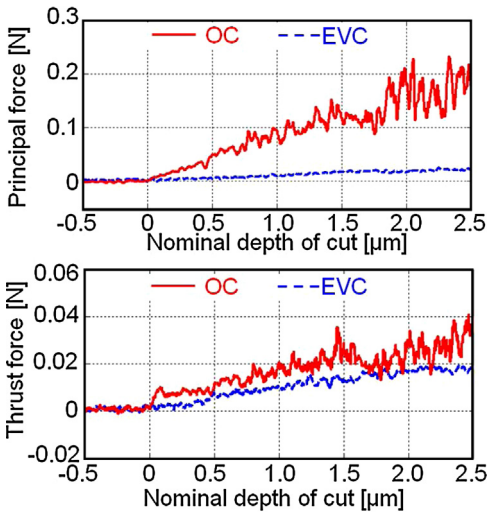

Fig. 4. Cutting force-nominal depth of cut curves in the EVC and OC grooving experiments.

200 mm/min. The amplitude in the nominal cutting direction and DOC direction in the EVC is 2 and 1 $\mu m_{0\text{-}p}$, respectively. Fig. 4 plots variations of cutting forces in the EVC and the OC grooving experiments, showing that both principal forces and thrust forces increase with increasing nominal DOC in the two types of cutting processes. However, the cutting forces in the EVC are generally much smaller than that in the OC due to thinner instantaneous uncut chip thickness in each elliptical vibration cycle [34,36,49]. In the EVC process, the principal force and thrust force are approximately equal to each other and are smoothly increased with increasing DOC, implying that the stable cutting process can be achieved even though in the brittle cutting of silicon by applying the EVC. In the OC process, the increase of principal force with increasing DOC is more sensitive than thrust force, which may be originated from different material removal modes. It's known that silicon is generally removed in the brittle mode in terms of crack initiation and propagation by applying the OC. Based on the fracture mechanism of brittle material reported by Griffith [52], the growth of a crack requires creation of two new surfaces, which leads to increased surface energy in the brittle cutting accompanied with slowly increased thrust force [31]. On the other hand, the material removal ratio increases with increasing DOC, accompanied with the rapid increase of principal force.

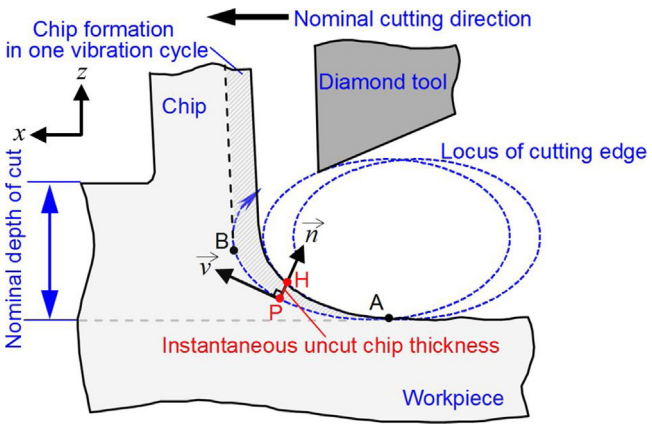

Fig. 6. Kinematic model of the EVC process.

Fig. 5(a) and (b) present microphotographs of grooves machined at a nominal depth of cut of 0.4 μm through the OC and the EVC, respectively. While the groove formed by the OC is filled with brittle fractures, a smooth surface can be obtained successfully by applying the EVC in ductile cutting. The nominal critical DOC in the EVC is 475 nm, which is 12.5 times higher than the critical DOC of 38 nm in the OC. It should be noted that the value of critical DOC in the current OC process is much smaller than the commonly reported value of about 100 nm due to a zero rake angle adopted in this work [16,34]. As indicated in Fig. 4, the smaller cutting forces in the EVC are much helpful to reduce lateral cracks in machining of brittle materials, which is also advantageous to suppress tool wear and decrease subsurface damage on machined surface [53].

Fig. 6 shows the kinematic model of the EVC process. At the beginning of cutting, the small part left in the former cycle is cut at a small depth, which leads to extremely thin instantaneous uncut chip thickness, as compared with the nominal DOC. The instantaneous uncut chip thickness at a position P can be numerally calculated based on instantaneous cutting direction and vector normal to the instantaneous cutting direction. The distance between the position P and the position H, which is the intersection position of the vector and the former vibration locus, is considered as the tiny instantaneous uncut chip thickness. Subsequently, the rake face of cutting tool contacts with formed chip in the former cycle. At this moment, the instantaneous uncut chip thickness is almost equal to the tool feed value along the nominal cutting direction in one vibration cycle. Due to the ultrasonic vibration frequency

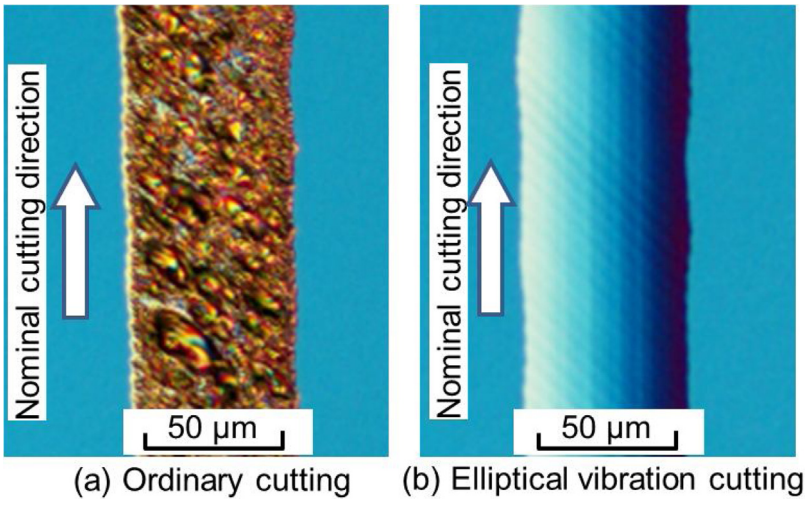

Fig. 5. Micro grooving of silicon by applying OC and EVC.

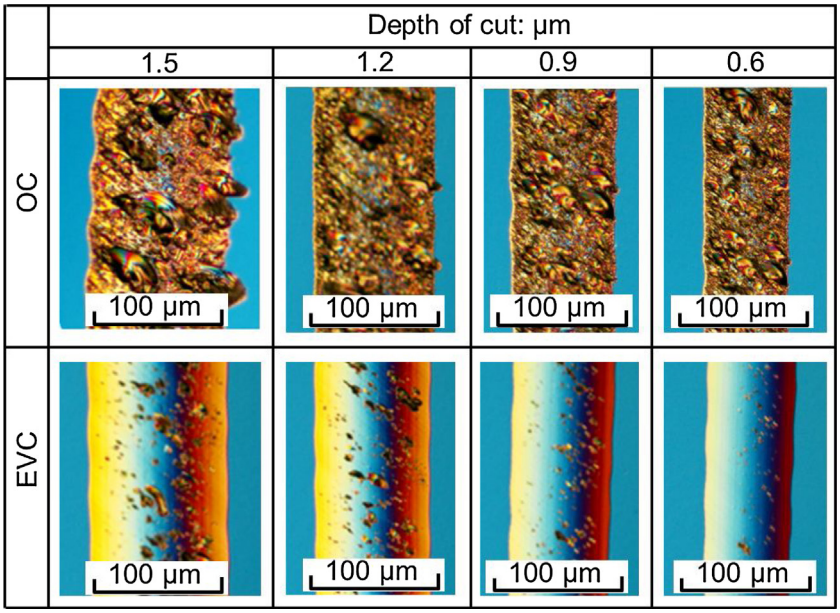

Fig. 7. Grooves formed by the OC and EVC in brittle cutting with different depth of cut.

and the small nominal cutting velocity, the instantaneous uncut chip thickness is almost within several tens of nanometers in actual cutting of brittle materials by applying the EVC [36,37]. Fractures initiate before pronounced permanent plastic deformation under conventional machining of silicon, due to its lower fracture strength than yield strength. However, with the extremely small instantaneous uncut chip thickness, very large stress can be achieved at small volumes, which triggers dislocation activities under high shear stress. Since the actual DOC is smaller than the critical value for ductile machining due to the size effect in fracture toughness of silicon, the EVC results in a significant improvement of the nominal critical DOC for ductile cutting of silicon. Especially, when the tool cuts the finished surface around the bottom of the elliptical vibration, the instantaneous uncut chip thickness decreases to several nanometers. Moreover, the actual rake angle acting on cutting regime becomes negative due to the tool moving up from the bottom of elliptical vibration locus, as shown in Fig. 1. It was reported by Komanduri et al. [54] and Yan et al. [55] that the negative rake angle can produce hydrostatic compressive pressure that is advantageous to suppress crack propagation and obtain ductile cutting of silicon.

Additionally, machined surfaces achieved by the EVC and OC in brittle cutting are also examined. Fig. 7 shows that the nominal DOC is gradually increased from 0.6 μm to 1.5 μm, which has a strong influence on machined surface quality for both types of cutting. However, the deterioration of machined surface quality in terms of formation of brittle defects is less pronounced in the EVC than the OC. Furthermore, the defect geometry is quite different in the EVC from that in the OC. While there are cleavage defects caused by the formation of continuous brittle defects on the whole machine surface observed in the OC, there are only discrete defects with smaller defect sizes generated in the EVC process. Even though at the largest DOC of 1.5 μm, the brittle defect propagation can also be efficiently suppressed and smooth side edges of grooves can be obtained by applying the EVC.

Fig. 8 shows the crack system in single edge cut of brittle materials that had been clarified previous [19,33]. This similar crack system is also reported by Marinescu [53] to clarify mechanisms for grinding of ceramics and estimate grinding rates. Two principal crack systems emanate from the plastic zone, i.e., median and lateral cracks, respectively. The median cracks are usually associated

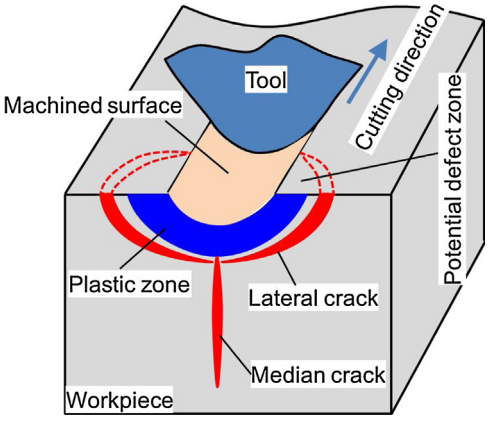

Fig. 8. Crack systems in single edge cut of brittle materials.

with strength degradation and the lateral cracks dominate material removal and surface formation. Deflection of lateral cracks toward free surface causes the material removal by brittle fracture. Based on experimental results shown in Fig. 7, it is confirmed that the propagation of lateral cracks inside the workpiece material can be efficiently suppressed by applying the EVC. Consequently, ductile deformation of silicon occurs with the prevention of crack propagation, i.e., transition of fracture from brittle cleavage to ductile tearing occurred, which is governed by either dislocation nucleation from the crack tip or the motion away of dislocations from the crack tip [56,57]. Although silicon is a one typical intrinsically brittle solid, its mechanical response subject to extreme applied load depends on the competition between different deformation modes [58]. In particular, the connection between dislocation mobility and ductile behavior of silicon has been demonstrated theoretically and experimentally [59–61].

Fig. 9 presents machined surface morphologies obtained in the EVC and OC with a small DOC of 0.6 μm. For the OC process, the generated defects are mainly in the size of about tens of micrometers and fulfilled with the whole coarse machined surface, suggesting that huge brittle defects are mainly caused by the lateral crack system. On the other hand, small pits with the size of about several micrometers are generated on the machined surface in the EVC,

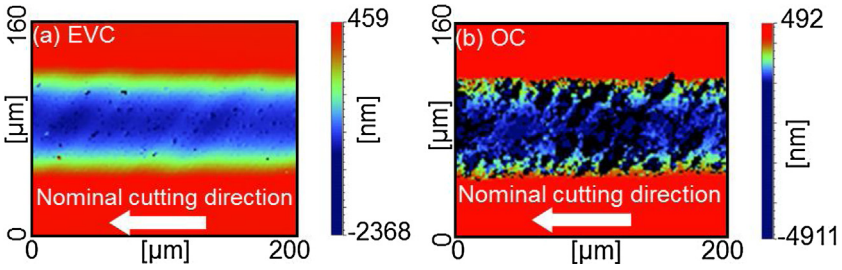

Fig. 9. Grooving surfaces in (a) EVC and (b) OC with a depth of cut of 0.6 μm.

which are primarily caused by the median crack system. Marinescu [53] indicated that the threshold load for median cracks is less than that for lateral cracks. With the small cutting forces shown in Fig. 4, the lateral cracks that cause huge brittle fracture can be successfully suppressed in the EVC process.

Fig. 10 further presents the atomic force microscope (AFM) images of machined surfaces obtained in the EVC and OC with a nominal DOC of 0.6 μm. The surface roughness Ra is about 20 nm and 181 nm for the EVC and the OC, respectively. The profile A-B indicated in Fig. 10 is measured along the nominal cutting direction. The maximum defect deepness is about 0.2 μm and 1.6 μm for the EVC and the OC, respectively. It is also important to note that part of the machined surface by applying the EVC possesses good surface integrity and smoothness even though in brittle cutting, which verifies the advantage of reducing crack propagation into machined surface of silicon by applying the EVC.

3.2. *Influence of vibration amplitudes on the machined surface quality*

Suzuki et al. [41] and Zhang et al. [36,62] reported that the vibration amplitude in the EVC process has a significant influence on ductile cutting of brittle materials. In the general EVC process, the nominal cutting speed v_c is usually set to be much lower than the maximum vibration speed v_{max} in the nominal cutting direction, which greatly restricts the machining efficiency. Based on the Eqs. (1) and (2), there is $v_{max} = A_c\omega$, where ω is the angular frequency of tool vibration and A_c is the mean-to-peak amplitude in the nominal cutting direction. With the present resonant 2-DOF elliptical vibrator, the angular frequency ω is fixed. In order to improve the machining efficiency, the maximum mean-to-peak vibration amplitude A_c of 2 $\mu m_{0\text{-}p}$ in the present vibrator is adopted. With changing of mean-to-peak vibration amplitude in the nominal DOC direction A_d, four vibration amplitudes A_c-A_d of 2-2 $\mu m_{0\text{-}p}$, 2-1 $\mu m_{0\text{-}p}$, 2-0.5 $\mu m_{0\text{-}p}$ and 2-0.25 $\mu m_{0\text{-}p}$ are adopted in the grooving experiments. A SCD tool with a nominal nose radius of 1 mm, a rake angle of 0° and a clearance angle of 10°, was used. The depth of cut is gradually increased from 0 μm to 1.5 μm. The nominal cutting speed is set to be 200 mm/min. In these grooving experiments, the speed ratio, i.e., the ratio of maximum vibration speed in the nominal cutting direction to the nominal cutting speed, is kept as a constant value of 156. Fig. 11 demonstrates the DBT position with different vibration amplitudes, which is defined as the nominal DOC for the continuous defect observation. It is indicated that with the vibration amplitudes A_c-A_d of 2-2 $\mu m_{0\text{-}p}$, 2-1 $\mu m_{0\text{-}p}$, 2-0.5 $\mu m_{0\text{-}p}$ and 2-0.25 $\mu m_{0\text{-}p}$, the according critical nominal DOC is about 193 nm, 456 nm, 495 nm and 261 nm, respectively.

It is experimentally confirmed that the critical nominal DOC can be efficiently improved by decreasing the vibration amplitudes from 2 $\mu m_{0\text{-}p}$ to 1 $\mu m_{0\text{-}p}$ in the DOC direction. When the vibration amplitude is large in the DOC direction, the slope of cutting edge trajectory becomes steep and chips pushed by the tool rake face become pronounced. Consequently, brittle fracture of silicon occurs easily due to its low fracture strength. In particular, funder a higher nominal depth of cut with a larger vibration amplitude in the vertical direction, the chip pulling-up-distance in vertical direction becomes longer. Massive silicon atoms may be torn off at one time from the workpiece surface by the pulling-up-motion and this large defect feature shown in Fig. 11(a) is not observed in OC. This phenomenon is considered to be specific problem in EVC [36]. Furthermore, with decreasing the vibration amplitude from 1 $\mu m_{0\text{-}p}$ to 0.5 $\mu m_{0\text{-}p}$ in the DOC direction, there is no significant difference in the value of critical nominal DOC. However, the brittle fracture occurs easily with a smaller vibration amplitude as increasing the nominal DOC. Especially when the nominal DOC is larger than the mean-to-peak amplitude in vertical direction, the brittle defects become significantly more serious with the vibration amplitude of 0.5 $\mu m_{0\text{-}p}$ in the DOC direction. With decreasing of the vibration amplitude in DOC direction, the pulling-up-motion of EVC process is decreased and the friction between the tool rake face and machined workpiece may be increased. These conditions finally increase the cutting forces and cause the easy brittle propagation [41]. In particular for the limit case in which the amplitude in the DOC direction becomes zero, the EVC process is changed into linear vibration cutting process (LVC). The instantaneous uncut chip thickness becomes the same as the nominal DOC in the OC process, which is disadvantageous in ductile machining of brittle materials [41]. For example, as shown in Fig. 11(d), the critical nominal DOC is decreased into 261 nm with a much small vibration amplitude of 0.25 $\mu m_{0\text{-}p}$ in the nominal DOC direction. Note that the defect feature becomes much more similar with that in the OC process with increasing the DOC. As compared with the machined surface with the vibration amplitude of 2 $\mu m_{0\text{-}p}$ in Fig. 11(a), the large defects-induced surface deterioration is not observed with the small vibration amplitude of 0.25 $\mu m_{0\text{-}p}$ due to the reduced chip pulling-up-motion. With these experimental and analytical investigations, a large vibration amplitude in the DOC direction can pull up and tear off the workpiece material easily. In contrast, a small vibration amplitude in the DOC direction can increase the instantaneous uncut chip thickness and cutting forces in each vibration cycle. Therefore, the appropriate vibration amplitudes A_c-A_d of 2-1 $\mu m_{0\text{-}p}$ and 2-0.5 $\mu m_{0\text{-}p}$ with larger critical nominal DOC can be applied to the ductile machining of silicon with a nominal cutting speed of 200 mm/min.

4. Fabrication of micro dimple structures

With the optimal machining conditions obtained in Section 3, the feasibility of sculpturing of silicon dimple microstructures by applying the amplitude-controlled sculpturing method in the EVC is clarified. The nominal DOC is regulated by controlling the vibration amplitude in the DOC direction. Because of this amplitude control, the nominal DOC can be changed rapidly without the conventional FTS. Fig. 12 shows the principle of the sculpturing method utilized in the EVC [48]. The envelope of the cutting edge trajectory is transferred into machined surface, resulting in the sculpturing of

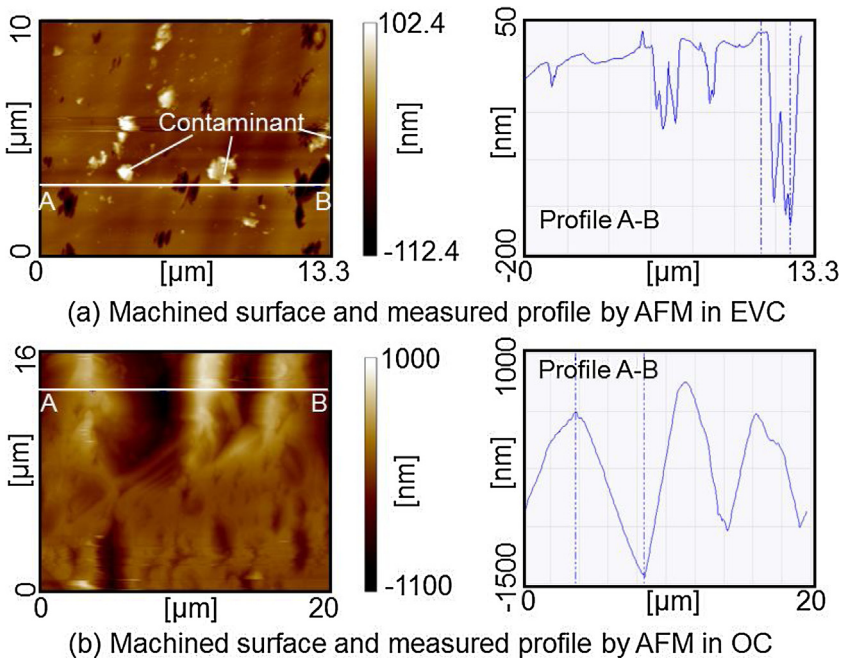

Fig. 10. Machined surface and measured profile by AFM in the EVC and the OC.

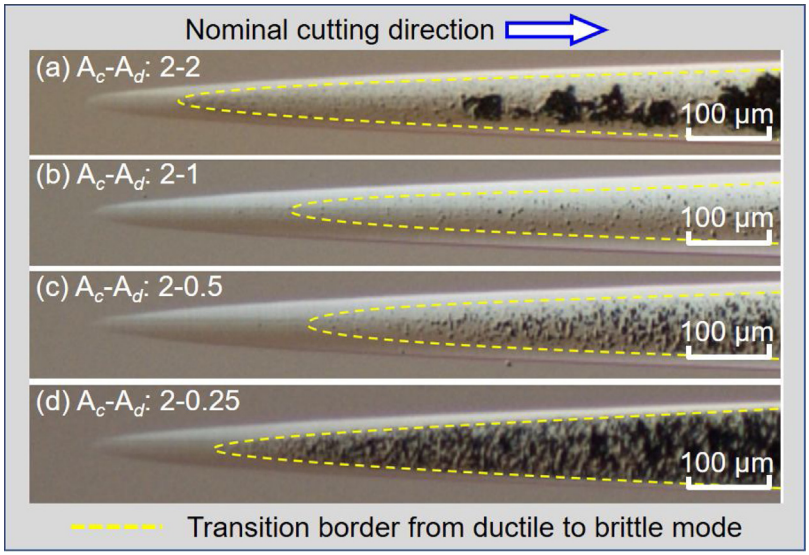

Fig. 11. Ductile-brittle transition position with different vibration amplitudes (A_c: Amplitude in nominal cutting direction, $\mu m_{0\text{-}p}$; A_d: Amplitude in depth of cut direction, $\mu m_{0\text{-}p}$).

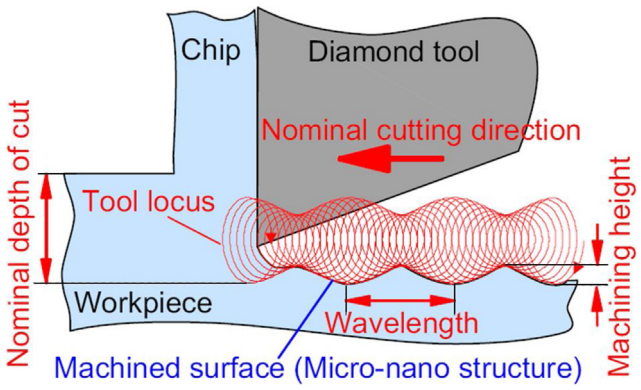

Fig. 12. Amplitude control sculpturing method in the EVC [48].

microstructures on the workpiece. The machining performance of microstructure fabrication on hardened steel and tungsten carbide was investigated elsewhere [48,63,64]. The vibration amplitude can be precisely controlled with a high resolution of several nanometers in the DOC direction.

In order to investigate the feasibility of the practical application, the proposed machining method was applied to a fabricate an angle grid surface [63,64] with sinusoidal structures on silicon. The structure height and wave length are 0.5 µm and 100 µm in both the nominal cutting direction and the nominal pick feed direction, respectively. A SCD tool with a nominal nose radius of 1 mm, a rake angle of 0° and a clearance angle of 10°, is utilized. The sinusoidal structure is machined with an amplitude command at 33.3 Hz in the nominal cutting direction. The mean-to-peak vibration amplitude is fixed to 2 $\mu m_{0\text{-}p}$ in the nominal cutting direction, while

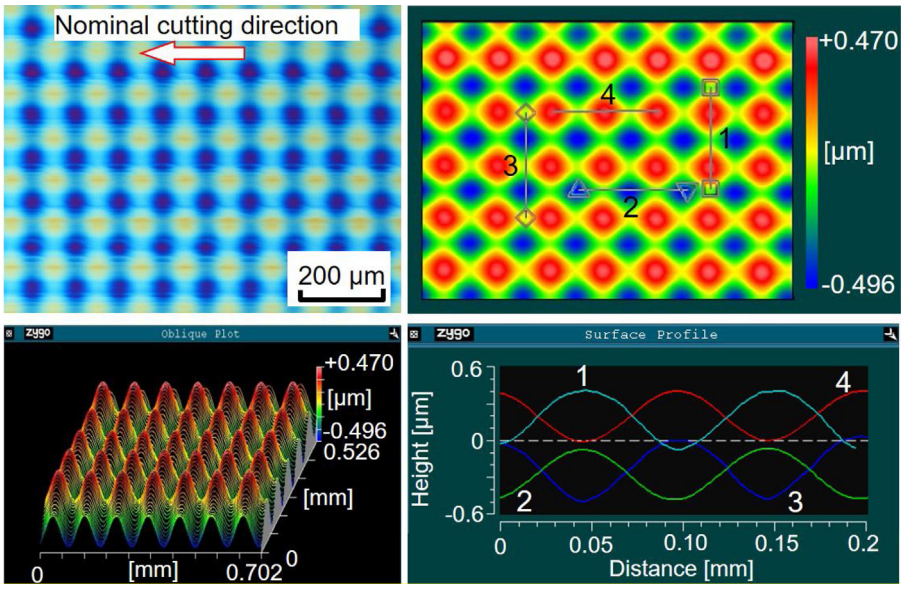

Fig. 13. Angle grid surface fabricated on silicon workpiece in ductile mode.

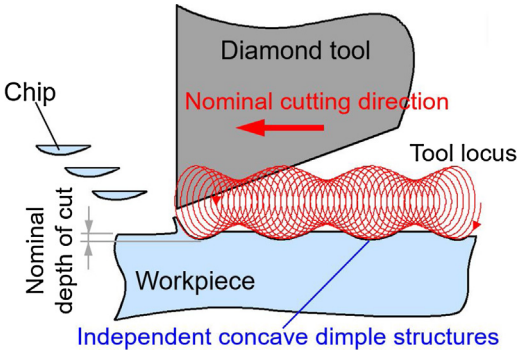

Fig. 14. Independent dimple structures fabrication with small nominal depth of cut.

varied within 0.5 $\mu m_{0\text{-}p}$-1 $\mu m_{0\text{-}p}$ in the DOC direction. The nominal cutting speed is set to be 200 mm/min, and the maximum DOC is adopted as 2 μm. On the other hand, the height position along the pick feed direction is controlled by utilizing positioning of the ultraprecision machine tool. The pick feed value is set to be 5 μm. The maximum effective depth of cut d_e is calculated to be 304 nm by the following equation [65]:

$$d_e = R - \sqrt{(R-d)^2 + \left(\sqrt{(2R-d)d} - f\right)^2} \quad (3)$$

where R is the tool radius, d is the maximum depth of cut and f is the pick feed value. Since the calculated maximum effective DOC is smaller than the critical DOC of 456 nm, the ductile sculpturing of silicon can be guaranteed by applying the above-mentioned machining conditions. Fig. 13 shows a microphotograph and a profile of the machined angle grid surface measured by optical microscope. It was confirmed that the periodic micro/nano structures with smooth surface can be successfully obtained in ductile mode. The machined height (0.483 μm) and the wavelength (100 μm) along the cutting direction and the pick feed direction correspond accurately to the pre-determined values.

Moreover, the independent concave dimples are also fabricated on the silicon workpiece. As shown in Fig. 14, the independent dimples can be fabricated with a small value of nominal DOC that is less than the mean-to-peak amplitude variation in the DOC direction.

In the present EVC process, the mean-to-peak amplitude in the nominal cutting direction is adopted as a stable value of 2 $\mu m_{0\text{-}p}$, and the vibration amplitude in the nominal DOC direction is appropriately controlled by sinusoidal wave and ramp wave, which is changed from 0.5 $\mu m_{0\text{-}p}$ to 1 $\mu m_{0\text{-}p}$ at 100 Hz. The nominal cutting speed is set to be 200 mm/min. As the critical nominal DOC is 456 nm with vibration amplitudes A_c-A_d of 2-1 $\mu m_{0\text{-}p}$, the maximum DOC should be less than the above-mentioned value in order to realize the ductile sculpturing process. Fig. 15 shows photographs of dimples sculptured on silicon. The maximum nominal DOC in the microstructure fabrication is set to be about 0.45 μm, which is less than the mean-to-peak amplitude variation of 0.5 μm. Consequently, the independent concave dimples with a maximum designed depth of about 0.45 μm are assumed to be machined in ductile cutting. The cross-section profile of the fabricated single pattern is measured by using a surface profiler (Taylor Hobson PGI 1250S). The measured structure height of the sinusoidal and ramp pattern is about 441 nm and 433 nm, respectively. The machining error along the nominal DOC direction is smaller than 20 nm for the current experimental setup. Therefore, it demonstrates the feasibility of high efficiency fabrication of high quality and high precision silicon microstructures by applying the amplitude-controlled sculpturing method in the EVC. The continuous development of the EVC process is expected to promote the development of sophisticated silicon microstructures in future industrial applications [66].

5. Conclusion

In the present work, we perform grooving experiments to investigate the ultra-precision machinability of silicon in ductile cutting by applying the EVC. With a nominal cutting speed of 200 mm/min and a vibration amplitude A_c-A_d of 2-1 $\mu m_{0\text{-}p}$, the critical nominal DOC for the silicon DBT is 475 nm, which is about 12.5 times higher than that of 38 nm in the OC. Even though there are brittle cracks generated in the EVC at a nominal DOC that is higher than the critical value, the dominant defect size is significantly smaller than that in the OC. Moreover, it is also revealed that the extremely small instantaneous uncut chip thickness and cutting forces achieved by applying the EVC are two advantageous factors to suppress the lateral crack propagation. It is found that the vibration amplitude in the nominal DOC direction A_d has a sig-

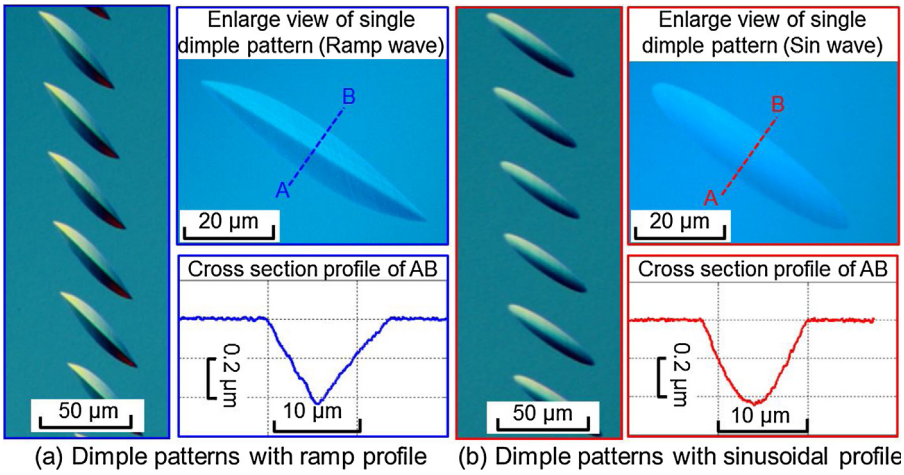

Fig. 15. Microphotograph and profiles of fabricated silicon dimple structures.

nificant influence on the ductile cutting of silicon. A large value of A_d can lead to easy pulling up and tearing off the workpiece material. On the other hand, a much small value of A_d can increase the instantaneous uncut chip thickness and cutting forces in each vibration cycle. Therefore, our experimental results indicate the optimal machining conditions for obtaining the ductile cutting of silicon in the EVC process: amplitudes A_c-A_d of 2-1 $\mu m_{0\text{-}p}$ and 2-0.5 $\mu m_{0\text{-}p}$, nominal cutting speed of 200 mm/min and nominal DOC of less than 456 nm. Based on the optimal machining conditions, high precision silicon microstructures of angle grid surface and independent concave dimple patterns are successfully sculptured on silicon through the EVC ductile cutting combined with the amplitude-controlled sculpturing method. Our experimental results demonstrate the feasibility of practical ultra-precision machining of silicon microstructures by applying the EVC.

Acknowledgments

The authors greatly acknowledge financial supports from the National Basic Research Program of China (Grant No. 2009ZX02005), the Specialized Research Fund for the Doctoral Program of Higher Education (20132302120038) and the Fundamental Research Funds for the Central Universities (HIT.NSRIF.2014050). Jianguo Zhang acknowledges the support from the Science and Technology Development Project of Jilin Province (20170520102JH) and the Knowledge Hub of Aichi.

References

[1] Chavoshi SZ, Goel S, Luo XC. Influence of temperature on the anisotropic cutting behaviour of single crystal silicon: a molecular dynamics simulation investigation. J Manuf Process 2016;23:201–10.
[2] Goel S, Luo XC, Agrawal A, Reuben RL. Diamond machining of silicon: a review of advances in molecular dynamics simulation. Int J Mach Tools Manuf 2015;88:131–64.
[3] Mohammadi H, Ravindra D, Kode SK, Patten JA. Experimental work on micro laser-assisted diamond turning of silicon (111). J Manuf Process 2015;19:125–8.
[4] Ayomoh M, Abou-El-Hossein K. Surface finish in ultra-precision diamond turning of single-crystal silicon. Proc SPIE/APOMA 2015;9633:96331.
[5] Chen YL, Cai YD, Shimizu Y, Ito S, Gao W, Ju BF. Ductile cutting of silicon microstructures with surface inclination measurement and compensation by using a force sensor integrated single point diamond tool. J Micromech Microeng 2016;26:025002.
[6] De CL, Kunzmann H, Peggs GN, Lucca DA. Surfaces in precision engineering, microengineering and nanotechnology. CIRP Ann-Manuf Technol 2003;52:561–77.
[7] Soref R. Mid-infrared photonics in silicon and germanium. Nat Photonics 2010;4:495–7.
[8] Mukaida M, Yan JW. Ductile machining of single crystal silicon for microlens arrays by ultraprecision diamond turning using a slow tool servo. Int J Mach Tools Manuf 2017;115:2–14.
[9] Brinksmeier E, Mutlugünes Y, Klocke F, Aurich JC, Shore P, Ohmori H. Ultra-precision grinding. CIRP Ann-Manuf Technol 2010;59:652–71.
[10] Sumitomo T, Huang H, Zhou L, Shimizu J. Nanogrinding of multi-layered thin film amorphous Si solar panels. Int J Mach Tools Manuf 2011;51:797–805.
[11] Sreejith P, Ngoi B. Material removal mechanisms in precision machining of new materials. Int J Mach Tools Manuf 2001;41:1831–43.
[12] Zong WJ, Sun T, Li D, Cheng K, Liang YC. XPS analysis of the groove wearing marks on flank face of diamond tool in nanometric cutting of silicon wafer. Int J Mach Tools Manuf 2008;48:1678–87.
[13] Albero J, Nieradko L, Gorecki C, Ottevaere H, Gomez V, Thienpont H, et al. Fabrication of spherical microlenses by a combination of isotropic wet etching of silicon and molding techniques. Opt Express 2009;17:6283–92.
[14] Ow YS, Breese MBH, Azimi S. Fabrication of concave silicon micro-mirrors. Opt Express 2010;18:14511–8.
[15] Pan A, Gao B, Chen T, Si J, Li C, Chen F, et al. Fabrication of concave spherical microlenses on silicon by femtosecond laser irradiation and mixed acid etching. Opt Express 2014;22:15245–50.
[16] Yan JW, Syoji K, Kuriyagawa T, Suzuki H. Ductile regime turning at large tool feed. J Mater Process Technol 2002;121:363–72.
[17] Venkatachalam S, Li XP, Liang SY. Predictive modeling of transition undeformed chip thickness in ductile-regime micro-machining of single crystal brittle materials. J Mater Process Technol 2009;209:3306–19.
[18] Fang FZ, Venkatesh VC. Diamond cutting of silicon with nanometric finish. CIRP Ann-Manuf Technol 1998;47:45–9.
[19] Arif M, Zhang XQ, Rahman M, Kumar S. A predictive model of the critical undeformed chip thickness for ductile–brittle transition in nano-machining of brittle materials. Int J Mach Tools Manuf 2013;64:114–22.
[20] Blake PN, Scattergood RO. Ductile-regime machining of germanium and silicon. J Am Ceram Soc 1990;73:949–57.
[21] Arif M, Rahman M, San WY. A state-of-the-art review of ductile cutting of silicon wafers for semiconductor and microelectronics industries. Int J Adv Manuf Technol 2012;63:481–504.
[22] Yan JW, Asami T, Harada H, Kuriyagawa T. Fundamental investigation of subsurface damage in single crystalline silicon caused by diamond machining. Precis Eng 2009;33:378–86.
[23] Yan JW. Laser micro-Raman spectroscopy of single-point diamond machined silicon substrates. J Appl Phys 2004;95:2094–101.
[24] Yan JW, Syoji K, Tamaki J. Some observations on the wear of diamond tools in ultra-precision cutting of single-crystal silicon. Wear 2003;255:1380–7.
[25] Li XP, Cai MB, Rahman M, Liang S. Study of the upper bound of tool edge radius in nanoscale ductile mode cutting of silicon wafer. Int J Adv Manuf Technol 2010;48:993–9.
[26] Arefin S, Li XP, Rahman M, Liu K. The upper bound of tool edge radius for nanoscale ductile mode cutting of silicon wafer. Int J Adv Manuf Technol 2007;31:655–62.
[27] Li XP, He T, Rahman M. Tool wear characteristics and their effects on nanoscale ductile mode cutting of silicon wafer. Wear 2005;259:1207–14.
[28] Uddin MS, Seah KHW, Li XP, Rahman M, Liu K. Effect of crystallographic orientation on wear of diamond tools for nano-scale ductile cutting of silicon. Wear 2004;257:751–9.
[29] Goel S, Luo XC, Reuben RL. Wear mechanism of diamond tools against single crystal silicon in single point diamond turning process. Tribol Int 2013;57:272–81.
[30] Mir A, Luo XC, Sun JN. The investigation of influence of tool wear on ductile to brittle transition in single point diamond turning of silicon. Wear 2016;364–365:233–43.

[31] Choi DH, Lee JR, Kang NR, Je TJ, Kim JY, Jeon EC. Study on ductile mode machining of single-crystal silicon by mechanical machining. Int J Mach Tools Manuf 2017;113:1–9.
[32] Shamoto E, Moriwaki T. Study on elliptical vibration cutting. CIRP Ann-Manuf Technol 1994;43:35–8.
[33] Zhang XQ, Arif M, Liu K, Kumar AS, Rahman M. A model to predict the critical undeformed chip thickness in vibration-assisted machining of brittle materials. Int J Mach Tools Manuf 2013;69:57–66.
[34] Zhu ZW, To S, Xiao GB, Ehmann KF, Zhang GQ. Rotary spatial vibration-assisted diamond cutting of brittle materials. Precis Eng 2016;44:211–9.
[35] Suzuki N, Masuda S, Shamoto E. Ultraprecision machining of sintered tungsten carbide by applying ultrasonic elliptical vibration cutting. In: Proceedings of 4th Euspen International Conference. 2004. p. 187–8.
[36] Zhang JG, Suzuki N, Wang YL, Shamoto E. Fundamental investigation of ultra-precision ductile machining of tungsten carbide by applying elliptical vibration cutting with single crystal diamond. J Mater Process Technol 2014;214:2644–59.
[37] Suzuki N, Masuda S, Haritani M, Shamoto E. Ductile machining of brittle materials by applying elliptical vibration cutting. In: Proceedings of the CIRP 2nd International Conference on HPC. 2006. CD-ROM.
[38] Shamoto E, Moriwaki T. Ultaprecision diamond cutting of hardened steel by applying elliptical vibration cutting. CIRP Ann-Manuf Technol 1999;48:441–4.
[39] Suzuki N, Nakamura A, Shamoto E, Harada K, Matsuo M, Osada M. Ultraprecision micromachining of hardened steel by applying ultrasonic elliptical vibration cutting. In: Proceedings of International Symposium on Micromechatronics and Human Science. 2003. p. 221–6.
[40] Brinksmeier E, Gläbe R. Advances in precision machining of steel. CIRP Ann-Manuf Technol 2001;50:385–8.
[41] Suzuki N, Hino R, Masuda S, Shamoto E. Ultraprecision cutting of sintered tungsten carbide by applying elliptical vibration cutting-study on ductile cutting mechanics. J Jpn Soc Precis Eng 2006;72:539–45 (In Japanese).
[42] Moriwaki T, Suzuki H, Mizugaki J, Maeyasu Y, Higashi Y, Shamoto E. Ultraprecision cutting of Molybdenum by ultrasonic elliptical vibration cutting. Proceedings of the 19th Annual Meeting of the ASPE, vol. 19. 2004. p. 621–4.
[43] Song YC, Park CH, Moriwaki T. Mirror finishing of Co-Cr-Mo alloy using elliptical vibration cutting. Precis Eng 2010;34:784–9.
[44] Ammouri AH, Hamade RF. BUEVA: a bi-directional ultrasonic elliptical vibration actuator for micromachining. Intl J Adv Manuf Technol 2012;58:991–1001.
[45] Fang FZ, Zhang XD, Weckenmann A, Zhang GX, Evans C. Manufacturing and measurement of freeform optics. CIRP Ann-Manuf Technol 2013;62:823–46.
[46] Brinksmeier E, Gläbe R, Schonemann L. Review on diamond-machining processes for the generation of functional surface structures. CIRP J Manuf Sci Technol 2012;5:1–7.
[47] Zhou JB, Li L, Naples N, Sun T, Yi AY. Fabrication of continuous diffractive optical elements using a fast tool servo diamond turning process. J Micromech Microeng 2013;23:075010.
[48] Suzuki N, Yokoi H, Shamoto E. Micro/nano sculpturing of hardened steel by controlling vibration amplitude in elliptical vibration cutting. Precis Eng 2011;35:44–50.
[49] Shamoto E, Morimoto Y, Moriwaki T. Elliptical vibration cutting (2nd report, study on effects of vibration conditions). J Jpn Soc Precis Eng 1999;65:411–7 (In Japanese).
[50] Shamoto E, Suzuki N, Hino R. Analysis of 3D elliptical vibration cutting with thin shear plane model. CIRP Ann-Manuf Technol 2008;57:57–60.
[51] Suzuki N, Haritani M, Yang J, Hino R, Shamoto E. Elliptical vibration cutting of tungsten alloy molds for optical glass parts. CIRP Ann-Manuf Technol 2007;56:127–30.
[52] Griffith AA. The phenomena of rupture and flow in solids. Philos Trans R Soc Lond Ser A Contain Pap Math Phys Charact 1921;221:163–98.
[53] Marinescu ID. Chapter 3: mechanisms for grinding of ceramics. In: Handbook of Advanced Ceramics Machining. Florida, USA: CRC Press; 2007. p. 56–67.
[54] Komanduri R, Chandrasekaran N, Raft LM. Effect of tool geometry in nanometric cutting: a molecular dynamics simulation approach. Wear 1998;219:84–97.
[55] Yan JW, Yoshino M, Kuriagwa T, Shirakashi T, Syoji K, Komanduri R. On the ductile machining of silicon for micro electro-mechanical systems (MEMS), opto-electronic and optical application. Mater Sci Eng A 2001;297:230–4.
[56] Brede M, Hsia KJ, Argon AS. Brittle crack propagation in silicon single crystals. J Appl Phys 1991;70:758–71.
[57] Holland D, Marder M. Ideal brittle fracture of silicon studied with molecular dynamics. Phys Rev Lett 1998;80:746–9.
[58] Zhang JJ, Zhang JG, Wang ZF, Hartmaier A, Yan YD, Sun T. Interaction between phase transformations and dislocations at incipient plasticity of monocrystalline silicon under nanoindentation. Comput Mater Sci 2017;131:55–61.
[59] Sen D, Cohen A, Thompson AP, van Duin ACT, Goddard III WA, Buehler MJ. Direct atomistic simulation of brittle-to-ductile transition in silicon single crystals. MRS Proceedings 2010;vol. 1272, 1272-PP 04-13.
[60] Hirsch PB, Roberts SG. The brittle-ductile transition in silicon. Philos Mag A 1991;64:55–80.
[61] Hintsala E, Teresi C, Gerberich WW. Linking nanoscales and dislocation shielding to the ductile-brittle transition of silicon. Metall Mater Trans A 2016;47:5839–44.
[62] Zhang JG, Suzuki N, Shamoto E. Micro machining of binderless tungsten carbide by applying elliptical vibration cutting technology. In: Proceedings of The Japan Society for Abrasive Technology Conference (ABTEC). 2011. p. 109–14.
[63] Zhang JG, Suzuki N, Wang YL, Shamoto E. Ultra-precision nano-structure fabrication by amplitude control sculpturing method in elliptical vibration cutting. Precis Eng 2015;39:86–99.
[64] Gao W, Araki T, Kiyono S, Okazaki Y, Yamanaka M. Precision nano-fabrication and evaluation of a large area sinusoidal grid surface for a surface encoder. Precis Eng 2003;27:289–98.
[65] Moriwaki T, Shamoto E, Inoue K. Ultraprecision ductile cutting of glass by applying ultrasonic vibration. CIRP Ann-Manuf Technol 1992;41:141–4.
[66] Zhang JG, Cui T, Ge C, Sui YX, Yang HJ. Review of micro/nano machining by utilizing elliptical vibration cutting. Int J Mach Tools Manuf 2016;106:109–26.